Supplemental Material

STRESS-INDUCED H3S28 PHOSPHORYLATION MODULATES LOCAL HISTONE ACETYLATION LEVELS

Anna Sawicka, Dominik Hartl, Malgorzata Goiser, Oliver Pusch, Roman R Stocsits, Ido M Tamir, Karl Mechtler, Christian Seiser

Supplemental Methods

Histone peptides used for the pull-down assay and mass spectrometry analysis:

H3unmodified (3-20): H2N-TKQTARKSTGGKAPRKQLC-CONH2
H3S10phK14ac (3-20): H2N-TKQTARKS(ph)TGGK(Ac)APRKQLC -CONH2
H3unmodified (19-36): H2N-QLATKAARKSAPATGGVKKC-CONH2
H3S28ph (19-36): H2N-QLATKAARKS(ph)APATGGVKKC-CONH2

Histone peptide pull-down assay

For histone peptide pull down assays, 0.1 mg of synthetic peptides (peptide sequences are given above), corresponding to amino acids 3-20 and 19-36 of histone H3 (numbered from N-terminus of histone H3) with a C-terminal cysteine added were coupled to 40 μl (bed volume) of SulfoLink Coupling Resin (Thermo Scientific) according to the manufacturer's instructions. Peptide-coupled resin was incubated overnight at 4°C on a roller with 500 μg of nuclear extract (isolated from proliferating HeLa cells treated with 188.5 nM Anisomycin for 1 hour) diluted to 0.5 μg/μl in the binding buffer (20 mM Tris-HCl pH 8.0, 135 mM NaCl, 0.5% NP40, 10% glycerol). The beads were washed 3 times 20 mM Tris-HCl pH 8.0, 135 mM NaCl, 0.5% NP40, 10% glycerol, followed by two washes with 200 mM NaCl, 50 mM Tris-HCl pH 8.0, 0.1 % SDS, 0.1% NP40, 0.5% sodium deoxycholate. Bound proteins were eluted by heating at 95°C for 5 min in 20 μl of Laemmli Sample Buffer and analyzed by Western Blotting. All washing buffers as well as the binding buffer were supplemented with Complete Protease Inhibitor (Roche).

Mass spectrometry analysis

Histone pull down assay was performed as described above with the following changes: 1 mg of nuclear extract from HeLa cells treated for 1 h with 188.5 nM

anisomycin was used, together with 0.4 mg of synthetic peptides and 200 μl (bed volume) of SulfoLink Coupling Resin. Following 2 washes with 200 mM NaCl, 50 mM Tris-HCl pH 8.0, 0.1% SDS, 0.1% NP40, 0.5% sodium deoxycholate, the samples were washed 5 times with 20 mM Tris-HCl pH 8.0, 135 mM NaCl, 10% glycerol (without protease inhibitors) and 2 times with 150 mM NaCl. The samples were washed 3 times with 25 mM ammonium bicarbonate (ABC) and then resuspended in 30 μl of ABC, supplemented with 200 ng of LysC and incubated at 37°C for 4 h. The LysC fraction was taken out and the beads were resuspended in 30 μl of 100 mM glycine, pH 2.0. The glycine elution was repeated twice and all three elutions were pooled. Then both fractions, LysC and glycine fraction were subjected to alkylation and reduction followed by tryptic digestion with 200 ng of trypsin in 37°C overnight. The digest was terminated by adding 10 μl of 10% TFA. 50% of each fraction was pooled and run for 3 h on the Ultimate 3000 HPLC RSLC nano system (Thermo Scientific) coupled to Q Exactive mass spectrometer with Proxeon nanospray source. For peptide identification, the .RAW-files were loaded into Proteome Discoverer (version 1.4.0.288, Thermo Scientific) and MS/MS spectra were searched using Mascot 2.2.07 (Matrix Science) against the human Uniprot database with the FDR cutoff of 0.5% at PSM (peptide spectrum matches) level and minimum 2 peptides per protein. The complete list of identified proteins is contained in Supplemental Tables 7-9: Supplemental Table 7 contains the list of identified proteins and number of unique peptides, Supplemental Table 8 contains the coverage details and Supplemental Table 9 contains the PMS information.

Primers used for quantitation of gene expression:

mRNA_*Rpl13a*_F: GGAGAAACGGAAGGAAAAGG
mRNA_*Rpl13a*_R: ACAGGAGCAGTGCCTAAGGA
mRNA_*Dusp1*_F: CTCCAAGGAGGATATGAAGCG (Auger-Messier et al. 2013)
mRNA_*Dusp1*_R: CTCCAGCATCCTTGATGGAGTC

mRNA_*Optn*_F: GTGGCCGGACCTGTTACC
mRNA_*Optn*_R: CAAACAACAGGCGCTCTTCC
mRNA_*Ube2v2*_F: TATTGGGCCACCAAGGACAAA
mRNA_*Ube2v2*_R: TGATGGAGGAGCTTCTGGGTA
mRNA_*Mafk*_F: GAAGCGCTTGTGAAGAGTGC
mRNA_*Mafk*_R: CCTTCAATGCCTTGTTGGGC
mRNA_*Traf1*_F: CACCAATGTCACCAAGC
mRNA_*Traf1*_R: CAGGAGAGCATCGTATTC
mRNA_*Nfil3*_F: TTTCTTTTCCCCCTCACGGA
mRNA_*Nfil3*_R: CCTCGTCCTACAGACCGGAT
mRNA_*Ell*_F: GGAGTTACGGGTTGTCGTGT
mRNA_*Ell*_R: AGAGATGTGCCCTTGGCTTC
mRNA_*Tank*_F: TTGACCCTTGATGAACCACA
mRNA_*Tank*_R: ATCCCTTTCGTGATGCAGAG
mRNA_*Egr3*_F: GGTGACCATGAGCAGTTTGC
mRNA_*Egr3*_R: TCCATCACATTCTCTGTAGCCA
mRNA_*Fos*_F: ATCTGTCCGTCTCTAGTG
mRNA_*Fos*_R: GCTTGGAGTGTATCTGTC

Adapters and primers used for scRNA-seq:

3'adaptor_PE: 5'-/5Phos/rArGrATCGGAAGAGCGGTTCAGC/3ddC/ -3'
5'adaptor_PE: 5'rArCrArCrUrCrUrUrUrCrCrCrUrArCrArCrGrArCrGrCr
UrCrUrUrCrCrGrArUrCrU-3'

RT_Primer_PE (primer for reverse transcription):

5'- TCTCGGCATTCCTGCTGAACCGCTCTTCCGATCT -3'

Library amplification primers:

PE_PCR_Primer_1.0 (forward primer):

5'-AATGATACGGCGACCACCGAGATCTACACTCTTTCCCTACACG
ACGCTCTTCCGATCT-3'

PE_PCR_Primer_2.0 (reversed primer):

5'-CAAGCAGAAGACGGCATACGAGATCGGTCTCGGCATTCCTGC
TGAACCGCTCTTCCGATCT-3'

Antibodies used for Western Blotting and dot blots:

H3S28ph (Sigma, cat number H9908), dilution 1:1000
H3S10ph (Santa Cruz Biotechnology, cat number 8656R), dilution 1:5000
H3S10ph (Active Motif, cat number 39253), dilution 1:5000
Anti-histone H3 C-terminus (Abcam, cat number 1791), dilution 1:50000
Lamin A/C (clone 4C11, Active Motif, cat number 39287), dilution 1:500
MSK1 (Sigma, cat number M5437), dilution 1:2000
MSK2 (Bethyl, cat number A302-746A), dilution 1:2000
RNAPIIS5ph (Bethyl, cat number A300-655A), dilution 1:5000
RNAPIIS2ph (Bethyl, cat number A300-654A), dilution 1:5000

β-Actin (Sigma, cat number A5316), dilution 1:20000
HDAC1 (10E, Seiser Lab, available at Millipore cat number 06-720), dilution 1:500
HDAC2 (3F3, Seiser Lab, available at Millipore cat number 05-814), dilution 1:1000
14-3-3zeta (Santa Cruz Biotechnology, cat number sc-1019), dilution 1:1000
mSin3A (AK-11) (Santa Cruz Biotechnology, cat number sc-767), dilution 1:500
MTA1 (C-17) (Santa Cruz Biotechnology, cat number sc-9446), dilution 1:500

Antibodies used for chromatin immunoprecipitation:

H3S28ph (Sigma, cat number H9908), 4 μg of antibody, 100 μg of chromatin
RNAPIIS5ph (Bethyl, cat number A300-655A), 4 μl of antibody, 25 μg of chromatin
RNAPIIS2ph (Bethyl, cat number A300-654A), 4 μl of antibody, 25 μg of chromatin
H3S10ph (Santa Cruz Biotechnology, cat number 8656R), 4 μg of antibody, 50 μg of chromatin
H3S10ph (Seiser Lab), 10 μl of serum, 50 μg of chromatin
H3S10phK14ac (Seiser Lab), 10 μl of serum, 100 μg of chromatin
H3K9ac (Millipore, cat number 06-942), 4 μg of antibody, 25 μg of chromatin
H3K4me3 (Millipore, cat number 07-473), 4 μg of antibody, 25 μg of chromatin
H3K27ac (Abcam, cat number ab4729), 4 μg of antibody, 25 μg of chromatin
H4ac (Millipore, cat number 06-866), 4 μl of serum, 25 μg of chromatin
Histone H3 (Active Motif, cat number 61475), 4 μg of antibody, 25 μg of chromatin
p300 C-20 (Santa Cruz Biotechnology, cat number sc-585), 4 μg of antibody, 50 μg of chromatin
PCAF H-369 (Santa Cruz Biotechnology, cat number sc-8999), 4 μg of antibody, 50 μg of chromatin
Gcn5 H-75 (Santa Cruz Biotechnology, cat number sc-20698), 4 μg of antibody, 50 μg of chromatin
mSin3A (K-20) (Santa Cruz Biotechnology, cat number sc-994X), 4 μg of antibody, 25 μg of chromatin
HDAC1 (Abcam, cat number ab7028), 4 μg of antibody, 25 μg of chromatin
HDAC2 (Bethyl, cat number A300-705A), 4 μl of antibody, 25 μg of chromatin

Primers used for ChIP-qPCR:

Dusp1(+108)_F: GACTTAGGGCCACAGGACAC
Dusp1(+108)_R: AAGAAGGAGCGACAATCCAA
*Dusp1*_+2517_F: TGTTTGAGGCAGTTTCTTCG
*Dusp1*_+2517_R: TGAGGTATTTGGTTCTTCTATGAG
Optn(-170)_F: TCCAAGAGAGGCTCTATCCCTA
Optn(-170)_R: CCAAGAAATTTCCCAGACCA
Optn(+42126)_F: GCCCAGCACAGCAGTACTTT
Optn(+42126)_R: CCGGTGAGGCTATAAACCAA
Ube2v2(-234)_F: TTCCCTTGGACACACTGACA
Ube2v2(-234)_R: GTTGGTTCATCGGTTGTCCT
Ube2v2(+38949)_F: GCAGGCGATTACAAGTTCCT
Ube2v2(+38948)_R: CGGTGTCACAACAAGTGCTC
Fosl1(+123)_F: CCCCCGTGGTGCAAGTGGTT (Drobic et al. 2010)
Fosl1(+123)_R: TGGCGGCTGCGGTTCTGACT
Fosl1(-962)_F: TCACCAGACTCAGCCACTTAC (Drobic et al. 2010)
Fosl1(-962)_R: GCCATCATAACCCCCACT
Mafk(+581)_F: GCCAAGGTCCCATCCAACTCTG
Mafk(+581)_R: TGATTTCTCGCCGCACGCTC

Mafk(+9671)_F: GGGGTTCTCTGGGGCTTAG
Mafk(+9671)_R: CCTGTCTACTTCGTTCCTGTTC
Traf1(+2630)_F: GGTGCTGCCTCATTCTTACC
Traf1(+2630)_R: ACTTGCTCCTGCGATCCTTA
Traf1(+13803)_F: CCCCAGTATCCAGTGCAAAT
Traf1(+13803)_R: ACAGGGAAGACACGGTTTTG
Nfil3(+500)_F: CCGGATTTCAGGAAAATTGA
Nfil3(+500)_R: GACTCAACCCTCCCCTTAGC
Nfil3(+13547)_F: TCAAGAGATTCATAGCCACACAAC
Nfil3(+13547)_R: ACACAAGGACACCCAGACAG
Tank(+1023)_F: CCTTCTTGCGAAAAGCCATA
Tank(+1023)_R: AACGTGAGTAGGCGCCTTTA
Tank(+56840)_F: GTCAAGTTTCCGCCTATGG
Tank(+56840)_R: AAAGTTTCCTGGGTTGTCTC
Ell(+96)_F: AGGGTGTCGGTGTTC
Ell(+96)_R: AGGTATCGCCAGGTG
Ell(+38299)_F: TTGTTGAGTTTGAGTTCTGGGTAGG
Ell(+38299)_R: GGGTCTTTGTGTAGTCTTGTCTGTC

Detailed description of computational analysis

Unless specified otherwise, the analysis was performed using Mac OS X system version 10.6.8, R version 3.0.1 (R Development Core Team 2014) and Bioconductor version 2.12 (Gentleman et al. 2004). We used *Mus musculus* genome annotation from July 2007 (NCBI37/mm9) throughout all our analysis.

Mapping of short reads

Mapping of the short reads was performed by the CSF NGS unit. In the case of ChIP-seq experiments, following the quality control, short reads were mapped to the mouse genome using Bowtie version 12.5 (Langmead et al. 2009), allowing up to two mismatches and retaining reads that map to only one genomic location. Reads derived from the input samples were trimmed to 36 bp prior to the mapping.

Strand-specific full-length mRNA-seq reads were quality controlled and mapped to the mouse genome using TopHat (Trapnell et al. 2009) version 1.4.1 allowing for one mismatch per 18 bp segment and retaining only uniquely mapped reads.

Reads derived from scRNA-seq were first trimmed to 25 bp and then mapped to the mouse genome using TopHat (Trapnell et al. 2009) version 1.4.1 allowing for one mismatch per 18 bp segment and retaining only uniquely mapped reads.

Total number of uniquely mapped reads for each experiment is summarized in Supplemental Table 1.

ChIP-seq peak calling and annotation

ChIP-seq experiments were carried out with two biological replicates per condition (control and anisomycin treated cells) with the exception of input, where only one sample per condition was sequenced. Based on high correlations (see Supplemental Fig. 2), we pooled the replicates and pooled libraries were used throughout this study. ChIP-seq Peak calling was performed using MACS version 1.4.4 (Zhang et al. 2008) with a p value cut-off of 1e-10 and a shiftsize of 100. Only peaks showing FDR (false discovery rate) ≤ 0.05 and fold change ≥ 5 were considered for further analysis (for the numbers of significant peaks called in each pooled library see Supplemental Table 2). Due to unequal sizes of ChIP-seq and input libraries, prior to peak calling, the reads from input samples were randomly subsampled to match the number of tags in a given ChIP-seq sample: first, input data sets were shuffled twice (using Unix "shuf" command) and then a desired number of random reads was retrieved (with "shuf –n *number_of_reads*" Unix command). Peaks were assigned to genes based on RefSeq gene annotation from mm9 assembly of the mouse genome obtained from UCSC. RefSeq entries were attributed to gene symbols using kgXref table from UCSC table browser. For multiple RefSeq entries matching one gene symbol, the RefSeq accession corresponding to the longest transcript was retained, resulting in the list of 21608 RefSeq genes used throughout this study. Peaks called in histone modification ChIP-seq experiments were annotated using the ChIPpeakAnno

Bioconductor package (Zhu et al. 2010). A peak was assigned to a RefSeq gene only if the distance between the two features was less than 2 kb. The peaks called in the RNA Polymerase II ChIP-seq experiments we assigned to RefSeq genes only if they showed an overlap with those genes. Supplemental Table 3 contains the list of all RefSeq genes with peaks assigned to them ("TRUE"- peak assigned, "FALSE" - no peak assigned).

Detection of differentially expressed genes in mRNA-seq data and determination of gene expression levels

We performed mRNA-seq experiment in two biological replicates for each condition (control and anisomycin treated cells) and applied the "union" model of the htseq-count script (Anders 2010) to calculate the number of reads associated with each of 21608 mouse RefSeq genes for each sample. We used those counts to compute RPKM values for each gene and determined Spearman's correlation coefficient (ρ) for each set of biological replicates. Based on high correlation of the replicates (ρ= 0.97 for both conditions, see Supplemental Fig. 4A) we used the log-transformed mean of RPKM values for each condition to plot the distribution of gene expression levels using kernel density estimation (see Supplemental Fig. 4B). Based on this distribution we set the threshold for gene expression to 1 RPKM ($\log_2$RPKM equal to zero). This is consistent with previous studies, which estimated that the value of 1 RPKM corresponds to one transcript per cell (Mortazavi et al. 2008). The area of the plot between $\log_2$RPKM = 0 and max $\log_2$RPKM was divided into 3 bins and genes located in each bin were assigned a gene expression level corresponding to "lowly expressed genes", "moderately expressed genes" and "highly expressed genes".

Analysis of differentially expressed genes across the two conditions was performed using htseq-count and Bioconductor edgeR package (Robinson et al. 2010). Genes

that showed minimum two fold change in expression (adjusted p value ≤ 0.01) and RPKM value ≥ 1 (in anisomycin treated samples) were considered upregulated whereas genes displaying fold change ≤ 0.5 (adjusted p value ≤ 0.01) and RPKM value ≥ 1 (in control samples) were classified as downregulated (80 genes). The output of differential expression analysis for all mRNA-seq experiments is summarized Supplemental Tables 3 and 6. In both tables, “FC” stands for fold change in expression between the treated and control condition.

scRNA analysis

We performed scRNA sequencing in two biological replicates for both conditions. Following the alignment, we removed all unpaired reads and reconstructed the coordinates of scRNA fragments from the paired tags. Subsequently, we collapsed all the duplicated fragments and calculated FPKM values in annotated RefSeq genes extended 1 kb upstream of the TSS. Based on high correlation between the biological replicates (see Supplementary Fig. 12A) we pooled them and pooled libraries were further analyzed. The analysis of the scRNA fragment distribution in the mouse genome using RSeQC (Wang et al. 2012) showed that around 80% of the fragments align within the boundaries of annotated RefSeq genes (see Supplemental Fig. 12B). In order to examine the degree of bidirectional transcription we computed fragment density 500 bp around the TSS of 17837 mouse RefSeq genes that do not overlap any annotated RefSeq gene on the opposite strand (see Supplemental Fig. 12C) using HOMER (Heinz et al. 2010). Consistent with previously published data (Core et al. 2008) we find significant level of bidirectional transcription.

Data visualization

Average density plots were generated using HOMER (Heinz et al. 2010). For each ChIP-seq library, the reads were extended to 200 bp, the corresponding bedgraph file (normalized for the library size) was created using Bedtools version 2.17.0 (Quinlan and Hall 2010) and signal density was calculated in 100 bp bins. Heatmaps of normalized tag densities were created with HOMER (Heinz et al. 2010), using bedgraph files (generated as explained above) as input and displayed with Java TreeView (Saldanha 2004). The genes were sorted by the average expression level in ansomycin-treated cells prior to visualization. Each row of the heatmap represents the average signal of 53 genes. Sequencing tracks were visualized with the Gviz R package (Hahne F. 2013) using bigwig files generated from bedgraph files.

Pausing index calculation

Pausing index was calculated as the ratio of RNAPIIS5ph ChIP-seq reads mapped to the promoter region (from -250 to + 250 from the TSS) of a given gene vs RNAPIIS5ph ChIP-seq reads mapped to the gene body region (from + 500 bp to 1000 bp from the TSS). Genes with ratio ≥ 2 were considered as paused. Pausing index was determined for 11085 RefSeq genes that were at least 1 kb long with the minimal number of RNAPIIS5ph ChIP-seq reads in the promoter region equal to 4. The minimal number of RNAPIIS5ph ChIP-seq reads per promoter was estimated by calculating the median of RNAPIIS5ph ChIP-seq reads in 21608 random windows with the size of 500 bp. The number of random regions per chromosome was equal to the number of RefSeq genes per chromosome. Estimated pausing index correlated well with the amount of scRNA derived from a given TSS (Supplemental Fig. 12E), as previously described (Nechaev et al. 2010).

Promoter classification based on the CpG content

CpG content was calculated as previously described (Mohn et al. 2008). Sequences derived from 1.5 kb regions upstream of the TSSs of 21608 RefSeq genes (promoter regions) were extracted and the CpG observed vs expected ratios (CpG_observed/expected) were calculated in 500 bp sliding windows (with 1 bp shift between the windows). Promoter classification was based on the 500 bp window with the highest ratio of CpG observed vs expected. CpG poor promoters: CpG_observed/expected < 0.45, CpG weak promoters: CpG_observed/expected 0.45-0.8, CpG strong promoters: CpG_observed/expected > 0.8.

Agilent microarray analysis

Total cellular RNA was isolated as described above. RNA labeling, hybridization to Agilent Whole Mouse 4x44k expression array (G2514F) as well as microarray scanning and raw data processing was performed by Source BioScience GmbH.

Microarray data analysis was performed using the LIMMA package (Smyth 2005). gProcessedSignals were quantile normalized and p-values were calculated by fitting a linear model (lmFit) and estimating p-values per probe using eBayes. In the case when multiple probes represented one RefSeq entry, the probe showing the highest significant fold change (p value after Benjamini & Hochberg adjustment < 0.05) was used in further analysis. RefSeq entries showing fold change ≥ 2 over control and p value after Benjamini & Hochberg adjustment < 0.05 were deemed upregulated.

Gene ontology (GO) analysis

The GO enrichment analysis was performed using DAVID (Huang da et al. 2009). p values (after Benjamini correction) were $\log_{10}$ transformed. Only significantly enriched categories are displayed (p values after the Benjamini correction < 0.05).

Transcription factor motif analysis

Known transcription factor motif enrichment analysis in promoters (-400 bp to +100 bp from the TSS) of genes upregulated upon 1 h anisomycin treatment was performed using HOMER (Heinz et al. 2010) findMotifsGenome.pl script. Promoter sequences of noninduced genes served as a background for differential enrichment analysis. p values were determined by the hypergeometric test. Top 5 enriched motifs are displayed.

Supplemental Figures (Suppl. Figs. 1-21)

Supplemental Figure 1. Determination of H3S28ph antibody specificity by dot blot analysis. (A, B) Differentially modified synthetic peptides with the sequence corresponding to amino acids 19-36 (in the case of peptides containing S28 residue) or 3-20 (in the case of peptides containing S10 residue) of histone H3 (numbered from N-terminus of histone H3) were probed with H3S28ph-specific antibody.

Supplemental Figure 2. Correlation of ChIP-seq biological replicates. Reads from both biological replicates were pooled and peak calling was performed as described in Supplemental Material. Subsequently, duplicated reads were collapsed and each read was extended to 200bp (which corresponds to the average DNA fragment length after sonication). RPM/peak was calculated for each sample individually and Spearman's correlation coefficient (ρ) was determined for each set of biological replicates. **(A)** H3S28ph ChIP-seq **(B)** H3K9ac ChIP-seq **(C)** H3K4me3 ChIP-seq **(D)** RNAPIIS5ph ChIP-seq and **(E)** RNAPIIS2ph ChIP-seq.

Supplemental Figure 3. Gene ontology biological processes categories overrepresented in genes showing stress-induced H3S28ph. x-axis values correspond to $\log_{10}$ transformed p values after the Benjamini correction. The top 10 enriched categories are shown.

Supplemental Figure 4. Correlation of mRNA-seq biological replicates and distribution of gene expression levels. (A) Normalized gene expression values (RPKM) were calculated for each mRNA-seq sample and Spearman's correlation coefficient (ρ) was determined for each set of biological replicates. **(B)** The

distribution of gene expression levels was determined by kernel density estimation of log_2-transformed average of RPKM values for the two biological replicates.

Supplemental Figure 5. Correlation between gene expression level and stress-induced H3S28ph. Normalized counts (RPKM) of H3S28ph ChIP-seq reads in anisomycin-treated dataset were calculated for 21608 RefSeq genes in the regions from –1 kb to +3 kb flanking the TSS. Spearman's correlation coefficient (ρ) was calculated to determine the correlation between normalized gene expression values (RPKM) and H3S28ph levels.

Supplemental Figure 6. Stress-induced H3S28ph targets genes associated with active histone modifications and bound by RNAPII. Heatmaps of normalized tag densities showing H3S28ph, H3K9ac and H3K4me3 signals as well as RNAPII occupancy in 6 kb (histone modifications) and 10 kb (RNAPII) windows surrounding the TSS. The genes are sorted by expression levels. Each row of the heatmap represents the average signal of 53 genes. Only expressed genes ($log_2RPKM \geq 0$) are shown.

Supplemental Figure 7. Stress-induced deposition of H3S28ph does not require active transcription. Cells were treated with anisomycin (A) in the absence or presence of the transcriptional inhibitors Actinomycin D or Triptolide. Untreated cells served as control (C). **(A)** Western blot analysis of H3S28ph levels. The H3 C-terminus antibody was used as loading control. **(B-E)** ChIP-qPCR analysis of stress-induced H3S28ph levels (left panels) and RT-qPCR expression analysis (right panels) for the *Dusp1, Mafk, Traf1* and *Nfil3* genes. Error bars represent SDs (n=3). (*) $p < 0.05$.

Supplemental Figure 8. Gene ontology molecular function categories enriched in genes upregulated by anisomycin treatment. x-axis values correspond to $\log_{10}$ transformed p values after the Benjamini correction. The top 10 enriched categories are shown.

Supplemental Figure 9. Genome browser representations of H3S28ph, H3K9ac, H3K4me3, RNAPIIS5ph and RNAPIIS2ph normalized tag density profiles of representative genes (*Traf1* and *Nfil3)* upregulated after 1 hour treatment with anisomycin. The profiles derived from untreated cells are depicted in blue and profiles of cells under stress-induced conditions are shown in red.

Supplemental Figure 10. Chemical inhibition of MSK1/2 activity as well as siRNA-mediated knockdown of MSK2 abolishes stress-induced H3S28ph and transcriptional induction. (A) Western blot analysis of stress-induced (A) H3S28ph levels upon the treatment with MSK1/2 inhibitor H89 as well as p38 kinase (upstream activator of MSK1/2) inhibitor SB203580. H3 C-terminus antibody was used to ensure equal loading. Untreated cells (C) served as control. **(B-D)** The efficiency of siRNA-mediated double knockdown of MSK1 and MSK2 and its effect on global stress-induced levels of H3S28ph. Western blot analysis of (**B**) MSK1 and (**C**) MSK2 protein levels upon siRNA-mediated knockdown in control cells (C) and anisomycin-treated cells (A). NT – stands for non-target siRNA control, MSK – stands for MSK1 and MSK2 siRNA; β-actin was used as loading control. (**D**) Western blot analysis of H3S28ph levels in MSK2 knockdown as well as siRNA non-target control cells upon 1 hour treatment with anisomycin. H3 C-terminus antibody was used to ensure equal loading. (**E** and **G**) ChIP analysis of H3S28ph at *Traf1* and *Nfil3* genes in control (C) and anisomycin-treated cells (A) in the absence and presence of H89 (left panels)

and RT-qPCR analysis of mRNA expression of *Traf1* and *Nfil3* genes in control (C) and anisomycin-treated cells (A) in the absence or presence of H89 (right panels). Error bars represent SDs (n=3). (*) $p < 0.05$. (**F** and **H**) ChIP-qPCR analysis of stress-induced H3S28ph in knockdown control (NT) and MSK2 knockdown (MSK) cells at *Traf1* and *Nfil3* genes (left panels) and RT-qPCR analysis of mRNA expression of *Traf1* and *Nfil3* genes upon anisomycin treatment in knockdown control (NT) and MSK2 knockdown (MSK) cells (right panels). Error bars represent SDs (n=3). (*) $p < 0.05$.

Supplemental Figure 11. Chemical inhibition of MSK activity with H89 affects stress-induced levels of RNAPII occupancy. ChIP-qPCR analysis of RNAPIIS5ph and RNAPIIS2ph occupancy at **(A)** *Dusp1*, **(B)** *Mafk,* **(C)** *Traf1* and **(D)** *Nfil3* genes in control (C) and anisomycin-treated cells (A) in the absence or presence of H89. Error bars represent SDs (n=3). (*) $p < 0.05$.

Supplemental Figure 12. Quality control of scRNA-seq data. (A) Biological replicates of scRNA libraries are highly correlated. FPKM values were calculated for RefSeq genes for regions from 1kb upstream TSS to TES and Spearman's correlation coefficient (ρ) was determined for each set of biological replicates. **(B)** Most (~80%) of sequenced scRNA fragments map within the boundaries of annotated RefSeq genes. Duplicated scRNA fragments reconstructed from uniquely mappable scRNA reads derived from paired-end sequencing (see Supplemental Methods section) were collapsed and their distribution over genomic features (CDS, 5'UTR, 3'UTR, Introns as well as regions 1 kb upstream the TSSs and 1 kb upstream the TESs) was analyzed using RSeQC. **(C)** The majority of sequenced scRNA fragments align to a sense strand (left panel – control, right panel – 1 hour

anisomycin). Fragment density in the region of 500 bp around the TSS was calculated for 17837 RefSeq genes that do not overlap with an annotated gene on the opposite strand. **(D)** RNAPIIS5ph ChIP-seq read number correlates well with scRNA read number in the regions from –250 bp to +250 bp flanking the TSSs of 11085 RefSeq genes with the minimal length of 1 kb and significant amounts of RNAPIIS5ph ChIP-seq reads mapped to the promoter region (see Supplemental Methods for details). Spearman's correlation coefficient (ρ) was calculated to determine the correlation between the two parameters. **(E)** scRNA read number in the regions from –250 bp to +250 bp flanking the TSSs correlates with the pausing index. 11085 RefSeq genes with the minimal length of 1 kb and significant amounts of RNAPIIS5ph ChIP-seq reads mapped to the promoter region were analyzed (see Supplemental Methods for details). Spearman's correlation coefficient (ρ) was calculated to determine the correlation between the two parameters.

Supplemental Figure 13. Transient deposition of the H3S28ph mark. ChIP-qPCR analysis of stress-induced H3S28ph at *Optn, Ube2v2, Ell* and *Tank* genes in control (C) and after 1, 3 and 6 hour anisomycin treatment (A). Error bars represent SDs (n=3). (*) $p < 0.05$.

Supplemental Figure 14. A subset of H3S28ph target genes is primed for later activation. (A) ChIP-qPCR analysis of stress-induced H3S28ph at *Ell* and *Tank* genes in control (C) and anisomycin-treated cells (A) in the absence or presence of H89. Error bars represent SDs (n=3). (*) $p < 0.05$. **(B)** RT-qPCR analysis of *Ell* and *Tank* gene expression after 1, 3 and 6 hour anisomycin treatment in the absence or presence of H89. Error bars represent SDs (n=3). (*) $p < 0.05$.

Supplemental Figure 15. Correlation of mRNA-seq biological replicates for 3 and 6 hours of anisomycin treatment in the presence or absence of H89. Normalized gene expression values (RPKM) were calculated for each mRNA-seq sample and Spearman's correlation coefficient (ρ) was determined for each set of biological replicates.

Supplemental Figure 16. Signaling-dependent histone acetylation at the H3S28ph target promoters. ChIP-qPCR analysis of H3K9ac, H3K27ac and H4ac levels at *Mafk, Optn, Tank* and *Ell* genes in control (C) and anisomycin-treated cells (A) in the absence or presence of H89. Error bars represent SDs (n=3). (*) $p < 0.05$.

Supplemental Figure 17. Analysis of H3K4me3 levels at the promoters of H3S28ph target genes. ChIP-qPCR analysis of H3K4me3 levels at *Dusp1*, *Ube2v2*, *Mafk, Optn, Ell* and *Tank* genes in control (C) and anisomycin-treated cells (A) in the absence or presence of H89. Error bars represent SDs (n=3). (*) $p < 0.05$.

Supplemental Figure 18. H3S28ph reduces the affinity of HDAC-containing complexes with histone H3 tail. Table summarizing the factors showing differential binding preferences towards H3(19-36) peptides either unmodified or phosphorylated at S28 identified by mass spectrometry analysis. The complete set of identified proteins is contained in the Supplemental Tables 7-9.

Supplemental Figure 19. Stress-induced H3S28ph reduces the association of HDAC-containing complexes with chromatin. ChIP-qPCR analysis of changes in SIN3A, HDAC2 and HDAC1 association with *Mafk*, *Optn*, *Ell* and *Tank* genes upon 1 hour anisomycin treatment (A) in the absence or presence of the MSK1/2 inhibitor

H89. Untreated cells served as control (C). Error bars represent SDs (n=3). (*) $p < 0.05$.

Supplemental Figure 20. Association of histone acetyltransferases with stress target promoters. ChIP-qPCR analysis of EP300, KAT2A and KAT2B occupancy at *Dusp1*, *Ube2v2*, *Mafk*, *Optn, Ell and Tank* genes upon 1 hour anisomycin treatment (A) in the absence or presence of MSK1/2 inhibitor H89. Untreated cells (C) served as a control. Error bars represent SDs (n=3). (*) $p < 0.05$.

Supplemental Figure 21. **Changes in transcriptional activation of stress-induced genes upon HDAC2 knockdown. (A)** The efficiency of HDAC2 knockdown. Western blot analysis of HDAC2 protein levels upon shRNA-mediated knockdown. NT – stands for non-target shRNA control, HD2 – stands for HDAC2 shRNA; β-actin was used as loading control. **(B-C)** RT-qPCR analysis of *Fos*, *Egr3*, *Ell*, and *Tank* gene expression upon anisomycin treatment (A) in control (NT) and HDAC2 (HD2) knockdown cells. Error bars represent SDs (n=3). (*) $p < 0.05$.

Supplemental Tables (1- 2, 4-5)

Supplemental Table 1. Number of uniquely mapped reads in ChIP-seq, RNA-seq and scRNA-seq experiments

	Experiment	Number of uniquely mapped reads [M]	Illumina platform/readlength/modus
ChIP-seq	H3S28ph_ctrl_replicate1	12.8	GAIIx/36bp/single-end
	H3S28ph_ctrl_replicate2	6.4	GAIIx/36bp/single-end
	H3S28ph_1hA_replicatete1	21.0	GAIIx/36bp/single-end
	H3S28ph_1hA_ replicate 2	14.1	GAIIx/36bp/single-end
	H3K9ac_ctrl_replicate1	22.4	GAIIx/36bp/single-end
	H3K9ac _ctrl_replicate2	38.8	GAIIx/36bp/single-end
	H3K9ac _1hA_replicate1	29.2	GAIIx/36bp/single-end
	H3K9ac _1hA_replicate2	31.3	GAIIx/36bp/single-end
	H3K4me3_ctrl_replicate1	14.9	GAIIx/36bp/single-end
	H3K4me3_ctrl_replicate2	31.1	GAIIx/36bp/single-end
	H3K4me3_1hA_replicate1	27.5	GAIIx/36bp/single-end
	H3K4me3_1hA_replicate2	18.7	GAIIx/36bp/single-end
	RNAPIIS5ph_ctrl_replicate1	15.7	GAIIx/36bp/single-end
	RNAPIIS5ph_ctrl_replicate2	11.6	GAIIx/36bp/single-end
	RNAPIIS5ph_1hA_replicate1	24.7	GAIIx/36bp/single-end
	RNAPIIS5ph_1hA_replicate2	6.3	HiSeq 2000/50bp/single-end
	RNAPIIS2ph_ctrl_replicate1	17.1	GAII/36bp/single-end
	RNAPIIS2ph_ctrl_replicate2	6.6	HiSeq 2000/50bp/single-end
	RNAPIIS2ph_1hA_replicate1	27.4	GAII/36bp/single-end
	RNAPIIS2ph_1hA_replicate2	9.8	GAII/36bp/single-end

	Input_ctrl	40.5	HiSeq 2000/50bp/ single-end
	Input_1hA	39.1	HiSeq 2000/50bp/single-end
scRNA-seq	scRNA_ctrl_replicate1	13.7 (sum)	GAIIx/76bp/paired-end
	scRNA_ctrl_replicate2	161.5 (sum)	HiSeq 2000/100bp/paired-end
	scRNA_1hA_replicate1	51.1 (sum)	GAIIx/76bp/paired-end
	scRNA_1hA_replicate2	66.2 (sum)	HiSeq 2000/100bp/paired-end
mRNA-seq -1	mRNA_ctrl_replicate1	41.1	HiSeq 2000/50bp/single-end
	mRNA_ctrl_replicate2	38.9	HiSeq 2000/50bp/single-end
	mRNA_1hA_replicate1	38.5	HiSeq 2000/50bp/single-end
	mRNA_1hA_replicate2	47.2	HiSeq 2000/50bp/single-end
mRNA-seq -2	mRNA_ctrl_replicate1	32.9	HiSeq 2000/50bp/single-end
	mRNA_ctrl_replicate2	26.1	HiSeq 2000/50bp/single-end
	mRNA_3hA_replicate1	35.7	HiSeq 2000/50bp/single-end
	mRNA_3hA_replicate2	30.9	HiSeq 2000/50bp/single-end
	mRNA_3hH89_replicate1	40.6	HiSeq 2000/50bp/single-end
	mRNA_3hH89_replicate2	50.9	HiSeq 2000/50bp/single-end
	mRNA_3hA+H89_replicate1	31.0	HiSeq 2000/50bp/single-end
	mRNA_3hA+H89_replicate2	30.8	HiSeq 2000/50bp/single-end
	mRNA_6hA_replicate1	29.5	HiSeq 2000/50bp/single-end
	mRNA_6hA_replicate2	24.6	HiSeq 2000/50bp/single-end
	mRNA_6hH89_replicate1	35.0	HiSeq 2000/50bp/single-end
	mRNA_6hH89_replicate2	34.3	HiSeq 2000/50bp/single-end
	mRNA_6hA+H89_replicate1	27.6	HiSeq 2000/50bp/single-end
	mRNA_6hA+H89_replicate2	29.3	HiSeq 2000/50bp/single-end

Supplemental Table 2. Number of peaks called in the ChIP-seq experiments

ChIP-seq	Number of called peaks
H3S28ph_ctrl	0
H3S28ph_1hA	4733
H3K9ac_ctrl	15247
H3K9ac_1hA	13704
H3K4me3_ctrl	10455
H3K4me3_1hA	12683
RNAPIIS5ph_ctrl	11784
RNAPIIS5ph_1hA	14979
RNAPIIS2ph_ctrl	9843
RNAPIIS2ph_1hA	9576

Supplemental Table 4. GO molecular function categories overrepresented in genes showing stress-induced H3S28ph. log_{10} transformed p values after the Benjamini correction are shown.

GO Molecular Function category term	$-log_{10}$(pvalue)
nucleotide binding	9.0
cytoskeletal protein binding	8.1
RNA binding	5.9
actin binding	5.7
purine ribonucleotide binding	5.6
ribonucleotide binding	5.6
zinc ion binding	5.3
metal ion binding	5.3
purine nucleotide binding	5.2
transition metal ion binding	5.2
cation binding	5.1
transcription activator activity	4.9
ion binding	4.8
adenyl ribonucleotide binding	4.7
transcription regulator activity	4.4
ATP binding	4.3
adenyl nucleotide binding	4.0
purine nucleoside binding	3.9
nucleoside binding	3.7
transcription factor binding	3.5
GTPase regulator activity	3.3
protein dimerization activity	3.1

nucleoside-triphosphatase regulator activity	3.1
transcription cofactor activity	2.8
protein kinase activity	2.7
growth factor binding	2.5
transcription repressor activity	2.5
enzyme activator activity	2.5
transcription coactivator activity	2.4
DNA binding	2.3
enzyme binding	2.3
small GTPase regulator activity	2.3
kinase binding	1.9
GTPase activator activity	1.7
microtubule binding	1.7
protein serine/threonine kinase activity	1.6
phospholipid binding	1.6
protein domain specific binding	1.4
tubulin binding	1.4

Supplemental Table 5. Gene ontology biological processes categories enriched in genes upregulated by anisomycin treatment. p values after the Benjamini correction were log_{10} transformed. Top 10 enriched categories are shown.

GO Biological Processes category term	- log_{10}(pvalue)
regulation of metabolic process	14.5
positive regulation of biological process	12.7
negative regulation of cellular process	12.5
negative regulation of biological process	12.4
positive regulation of cellular process	12.0
regulation of cellular process	11.2
regulation of developmental process	10.7
regulation of biological process	10.1
multicellular organismal development	9.6
regulation of multicellular organismal process	9.4

REFERENCES

Anders S. 2010. HTSeq: Analysing high-throughput sequencing data with Python. EMBL Heidelberg (Genome Biology Unit), Heidelberg, germany.

Auger-Messier M, Accornero F, Goonasekera SA, Bueno OF, Lorenz JN, van Berlo JH, Willette RN, Molkentin JD. 2013. Unrestrained p38 MAPK activation in Dusp1/4 double-null mice induces cardiomyopathy. *Circulation research* **112**(1): 48-56.

Brunmeir R, Lagger S, Simboeck E, Sawicka A, Egger G, Hagelkruys A, Zhang Y, Matthias P, Miller WJ, Seiser C. 2010. Epigenetic regulation of a murine retrotransposon by a dual histone modification mark. *PLoS genetics* **6**(4): e1000927.

Core LJ, Waterfall JJ, Lis JT. 2008. Nascent RNA sequencing reveals widespread pausing and divergent initiation at human promoters. *Science* **322**(5909): 1845-1848.

Drobic B, Perez-Cadahia B, Yu J, Kung SK, Davie JR. 2010. Promoter chromatin remodeling of immediate-early genes is mediated through H3 phosphorylation at either serine 28 or 10 by the MSK1 multi-protein complex. *Nucleic acids research* **38**(10): 3196-3208.

Gentleman RC, Carey VJ, Bates DM, Bolstad B, Dettling M, Dudoit S, Ellis B, Gautier L, Ge Y, Gentry J et al. 2004. Bioconductor: open software development for computational biology and bioinformatics. *Genome biology* **5**(10): R80.

Hahne F. DS, Ivanek R., Mueller A. and Lianoglou S.,. 2013. Gviz: Plotting data and annotation information along genomic coordinates. R package version 1.4.5. .

Heinz S, Benner C, Spann N, Bertolino E, Lin YC, Laslo P, Cheng JX, Murre C, Singh H, Glass CK. 2010. Simple combinations of lineage-determining transcription

factors prime cis-regulatory elements required for macrophage and B cell identities. *Molecular cell* **38**(4): 576-589.

Huang da W, Sherman BT, Lempicki RA. 2009. Systematic and integrative analysis of large gene lists using DAVID bioinformatics resources. *Nature protocols* **4**(1): 44-57.

Langmead B, Schatz MC, Lin J, Pop M, Salzberg SL. 2009. Searching for SNPs with cloud computing. *Genome biology* **10**(11): R134.

Mohn F, Weber M, Rebhan M, Roloff TC, Richter J, Stadler MB, Bibel M, Schubeler D. 2008. Lineage-specific polycomb targets and de novo DNA methylation define restriction and potential of neuronal progenitors. *Molecular cell* **30**(6): 755-766.

Mortazavi A, Williams BA, McCue K, Schaeffer L, Wold B. 2008. Mapping and quantifying mammalian transcriptomes by RNA-Seq. *Nature methods* **5**(7): 621-628.

Nechaev S, Fargo DC, dos Santos G, Liu L, Gao Y, Adelman K. 2010. Global analysis of short RNAs reveals widespread promoter-proximal stalling and arrest of Pol II in Drosophila. *Science* **327**(5963): 335-338.

Quinlan AR, Hall IM. 2010. BEDTools: a flexible suite of utilities for comparing genomic features. *Bioinformatics* **26**(6): 841-842.

R Development Core Team. 2014. R: A language and environment for statistical computing. R Foundation for Statistical Computing, Vienna, Austria. http://www.R-project.org/.

Robinson MD, McCarthy DJ, Smyth GK. 2010. edgeR: a Bioconductor package for differential expression analysis of digital gene expression data. *Bioinformatics* **26**(1): 139-140.

Saldanha AJ. 2004. Java Treeview--extensible visualization of microarray data. *Bioinformatics* **20**(17): 3246-3248.

Smyth G. 2005. Limma: linear models for microarray data. In: 'Bioinformatics and Computational Biology Solutions using R and Bioconductor'. R. Gentleman, V. Carey, S. Dudoit, R. Irizarry, W. Huber(eds). *Springer, New York*: 397-420.

Trapnell C, Pachter L, Salzberg SL. 2009. TopHat: discovering splice junctions with RNA-Seq. *Bioinformatics* **25**(9): 1105-1111.

Wang L, Wang S, Li W. 2012. RSeQC: quality control of RNA-seq experiments. *Bioinformatics* **28**(16): 2184-2185.

Zhang Y, Liu T, Meyer CA, Eeckhoute J, Johnson DS, Bernstein BE, Nusbaum C, Myers RM, Brown M, Li W et al. 2008. Model-based analysis of ChIP-Seq (MACS). *Genome biology* **9**(9): R137.

Zhu LJ, Gazin C, Lawson ND, Pages H, Lin SM, Lapointe DS, Green MR. 2010. ChIPpeakAnno: a Bioconductor package to annotate ChIP-seq and ChIP-chip data. *BMC bioinformatics* **11**: 237.

Sawicka_Suppl_Fig1.

αH3S28ph (Sigma, # H9908)

A

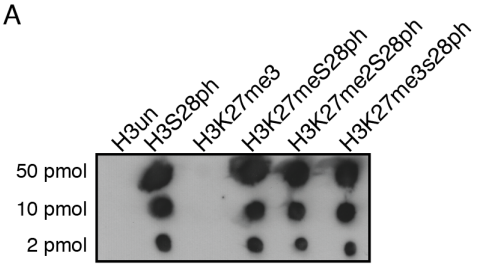

B

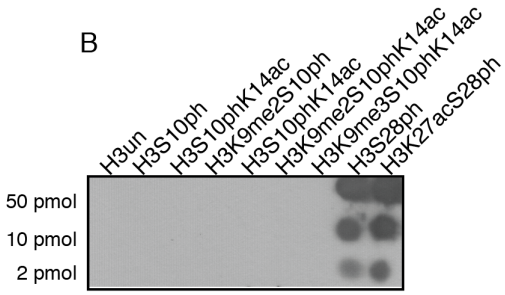

Sawicka_Suppl_Fig2.

A

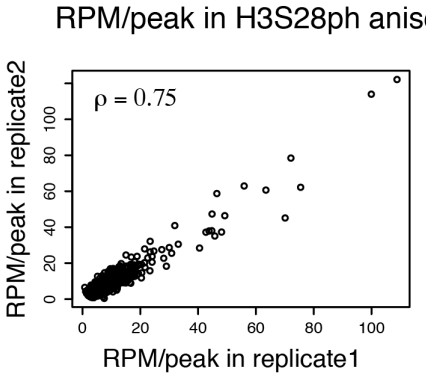

B

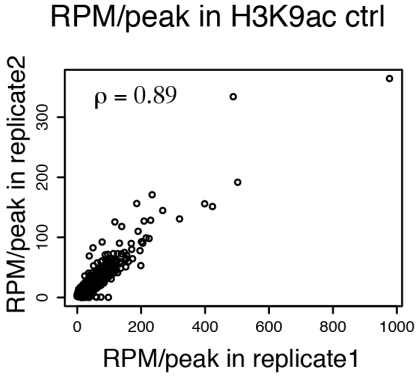

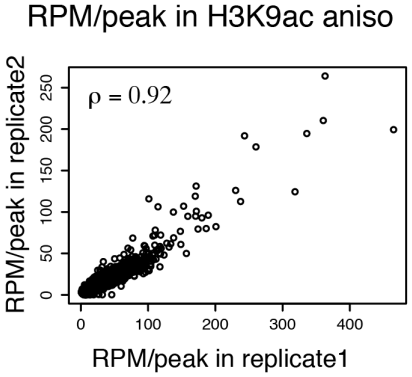

C

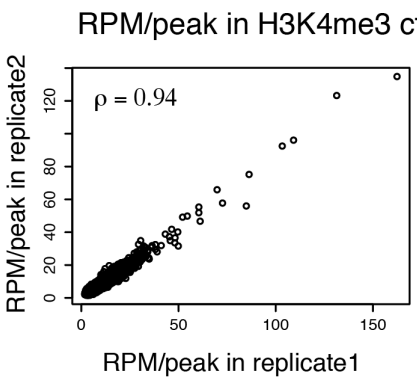

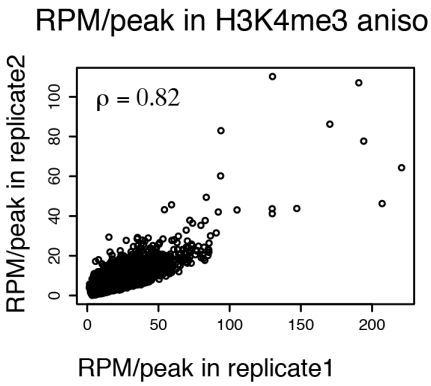

D

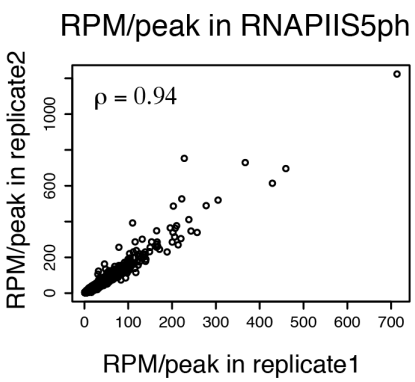

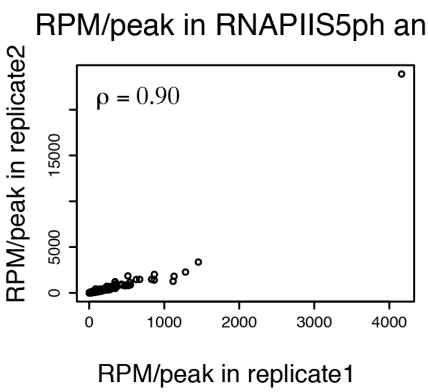

E

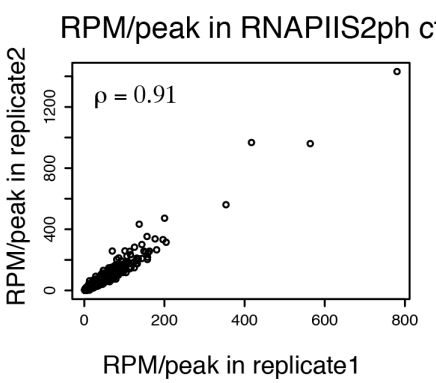

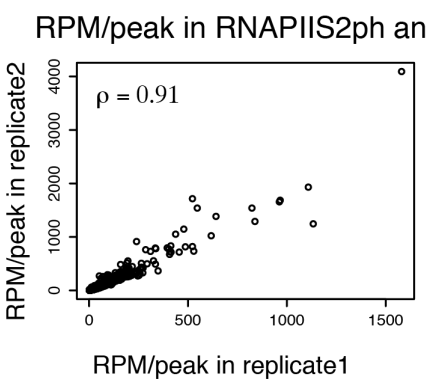

Sawicka_Suppl_Fig3.

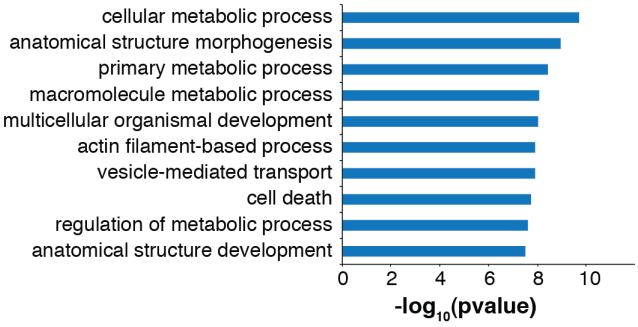

Sawicka_Suppl_Fig4

A

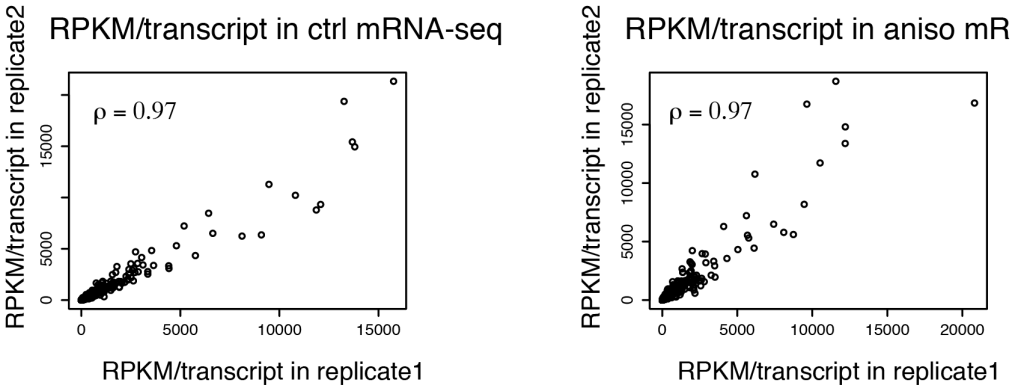

B

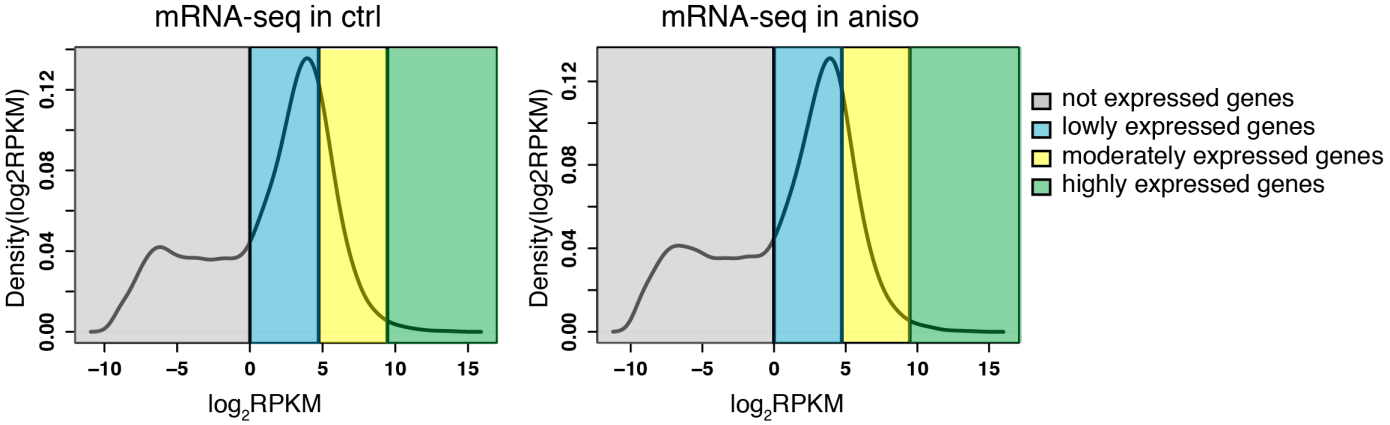

Sawicka_Suppl_Fig5

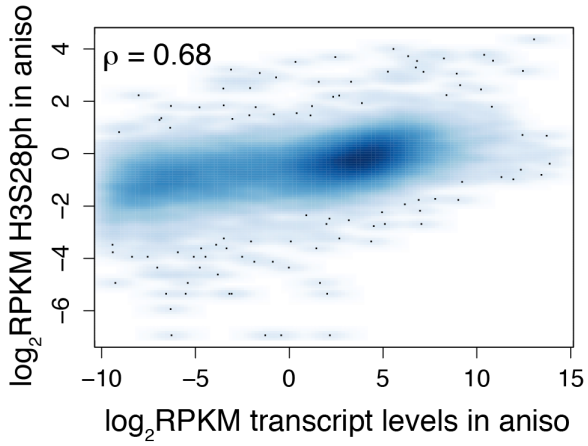

Sawicka_Suppl_Fig6

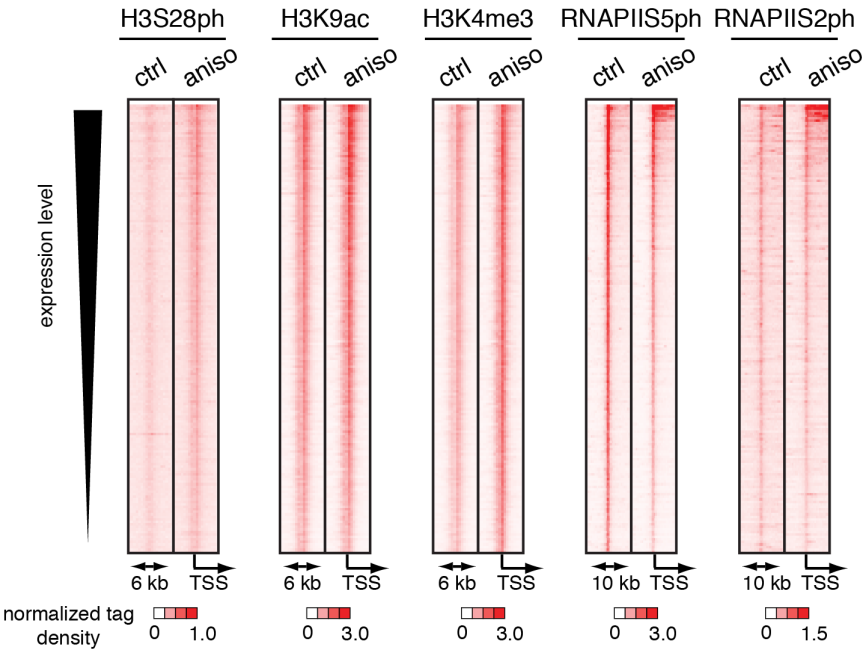

Sawicka_Suppl_Fig7

A

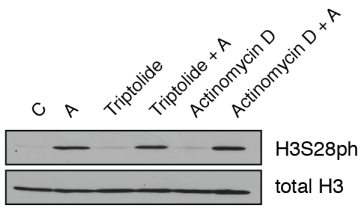

B

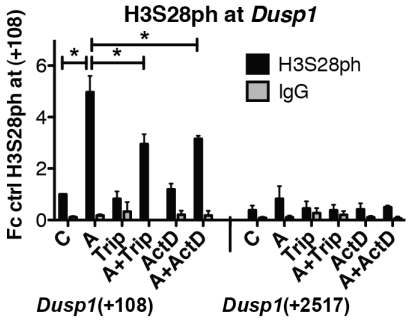

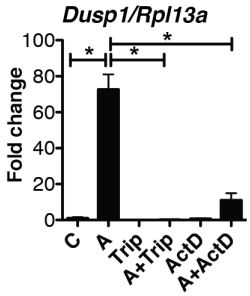

C

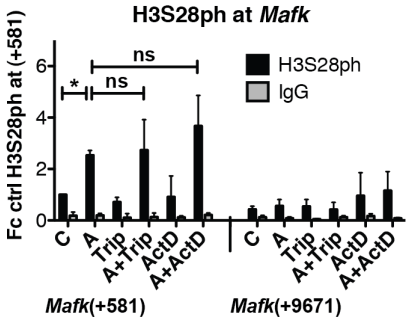

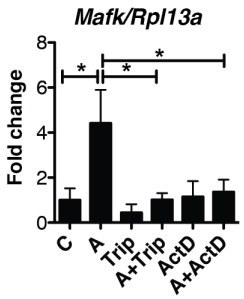

D

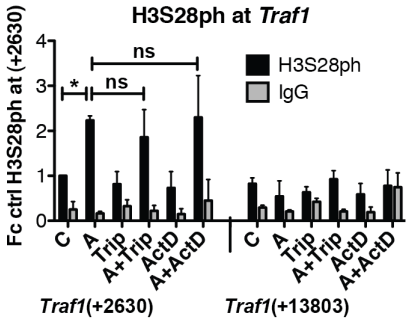

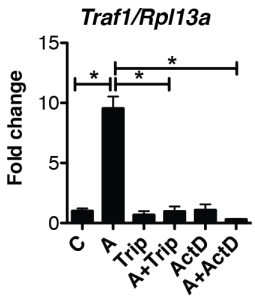

E

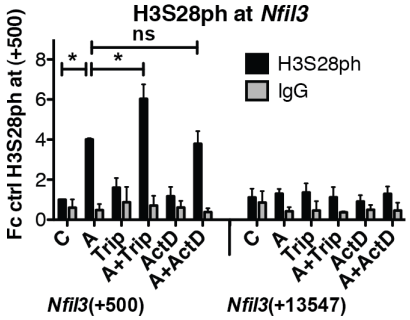

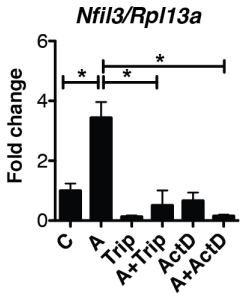

Sawicka_Suppl_Fig8

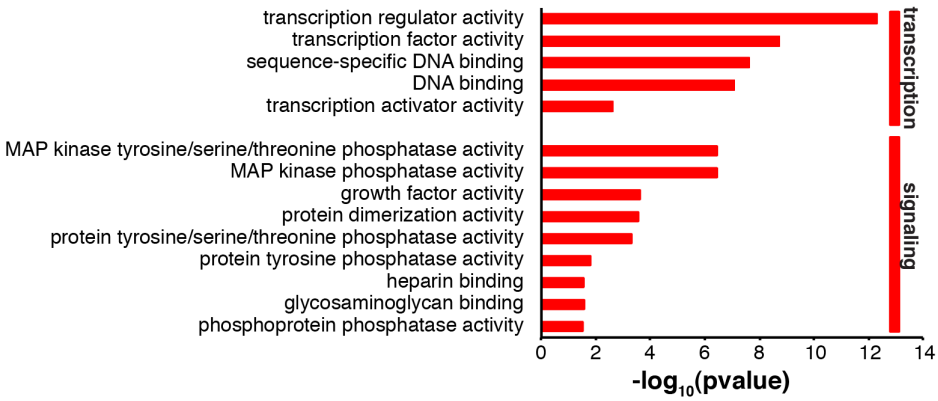

Sawicka_Suppl_Fig9

A

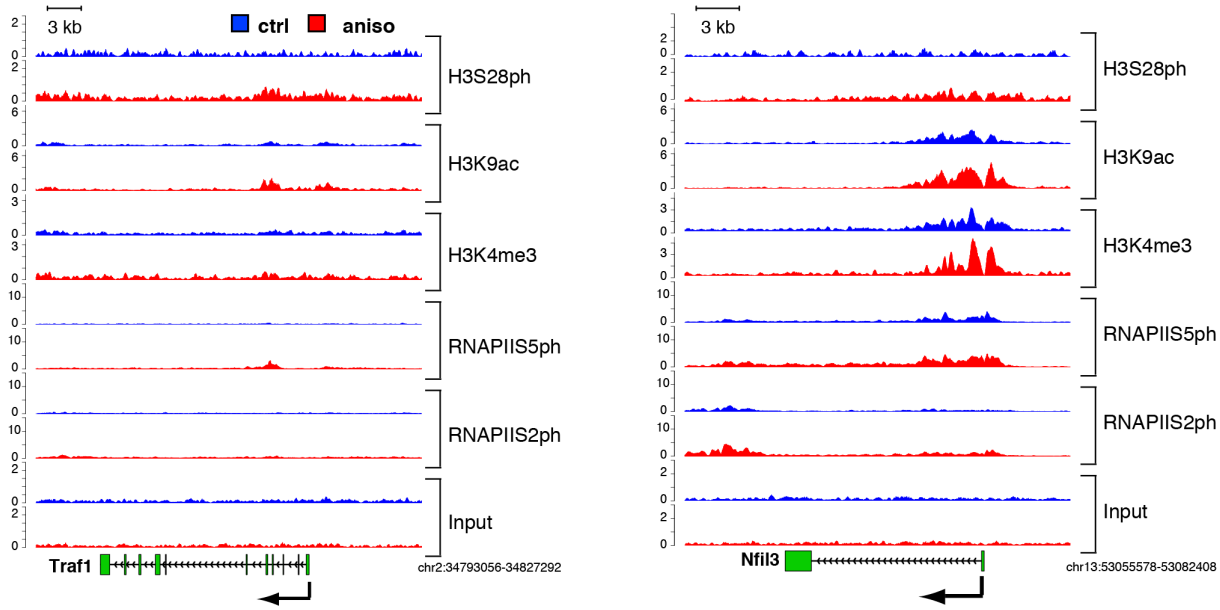

Sawicka_Suppl_Fig10

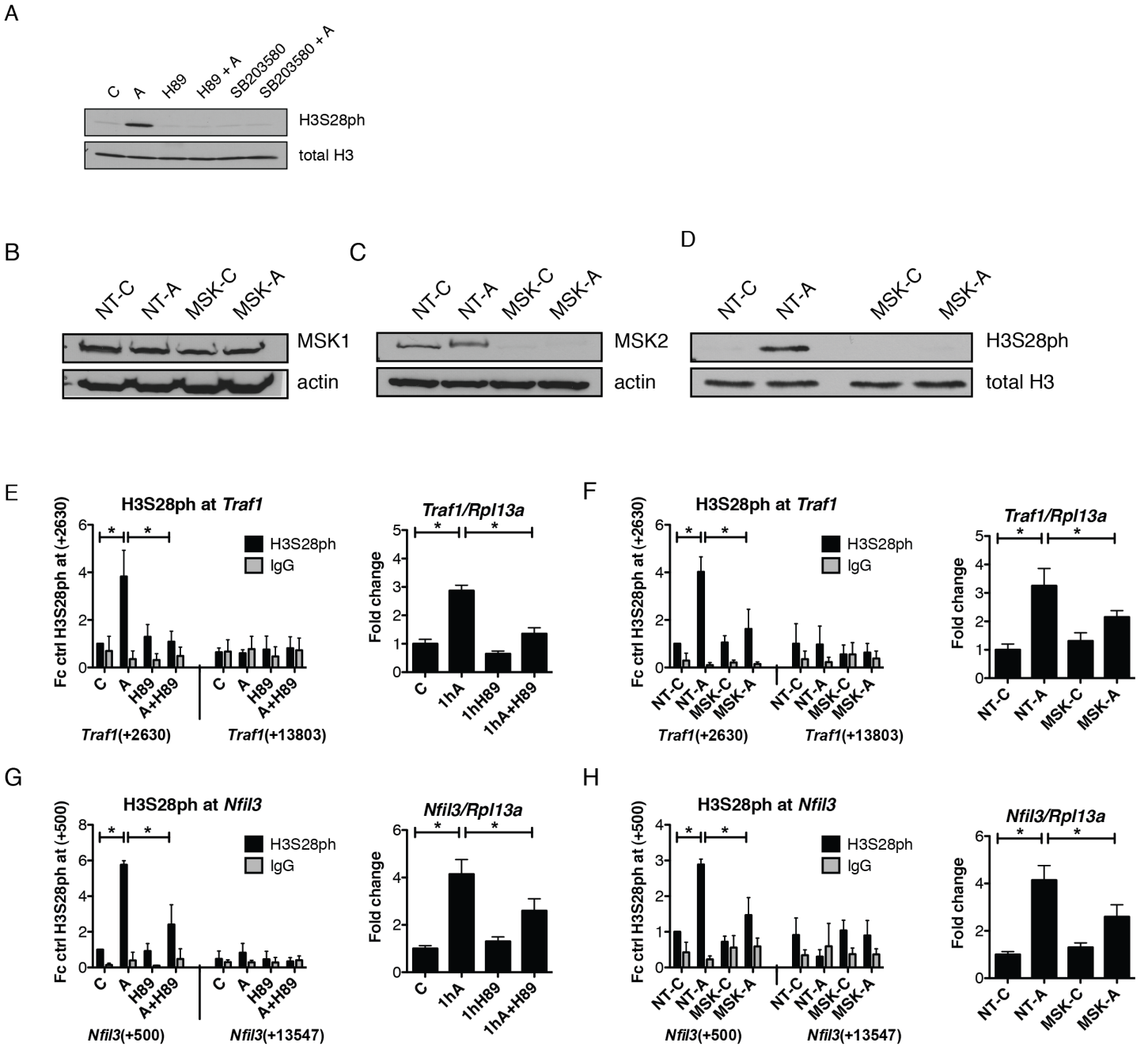

Sawicka_Suppl_Fig11

A

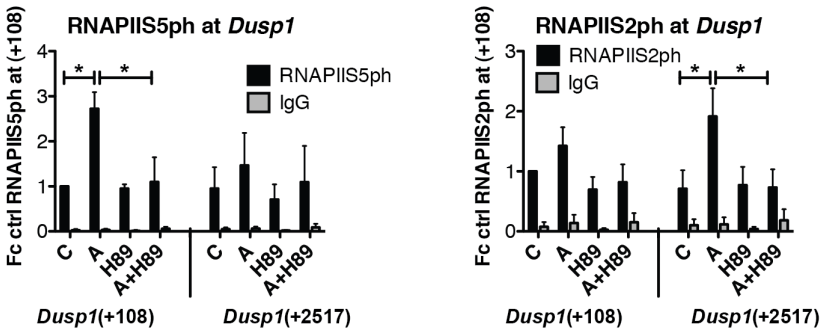

B

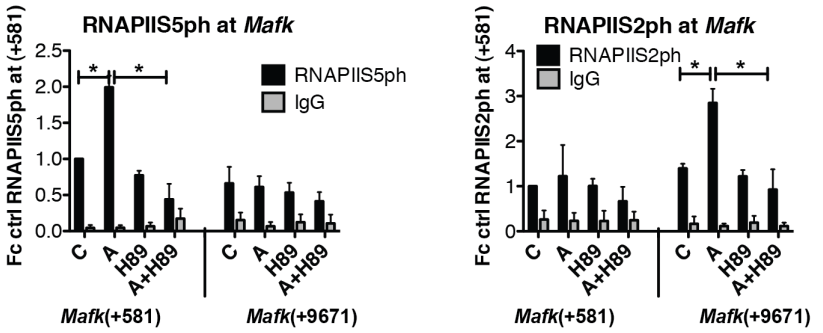

C

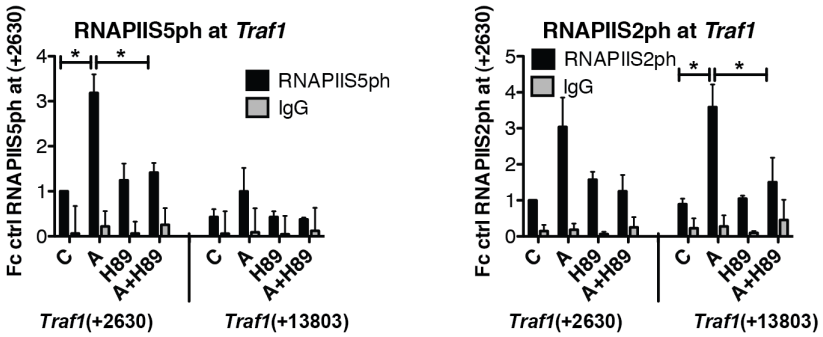

D

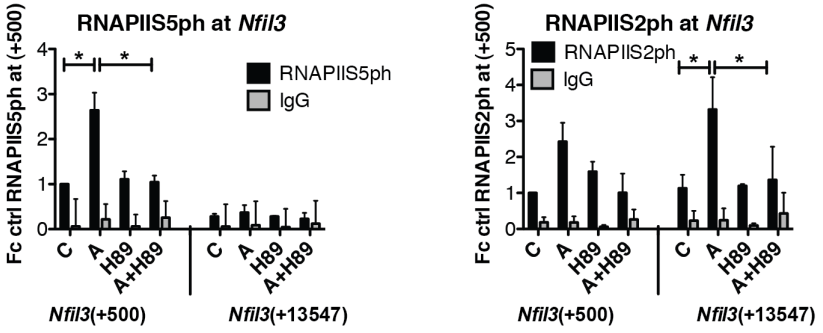

Sawicka_Suppl_Fig12

A

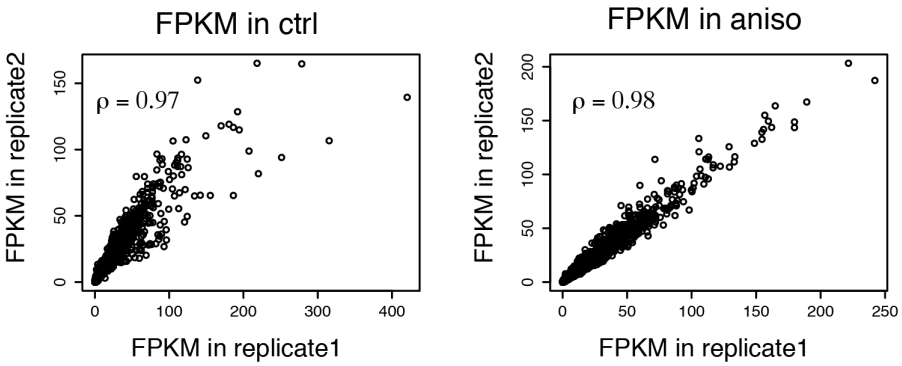

B

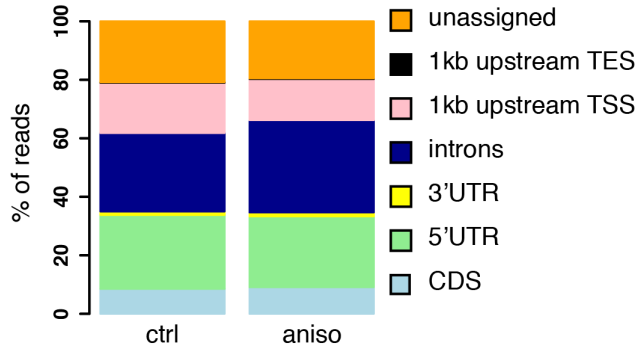

C

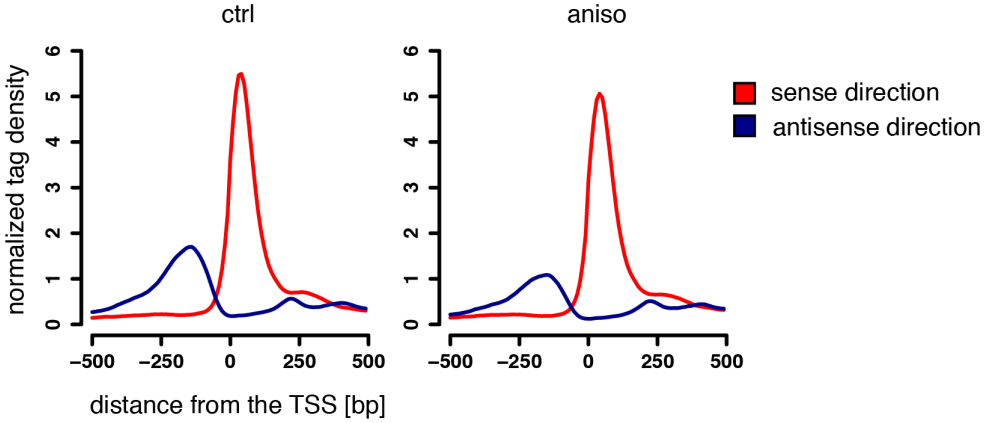

D

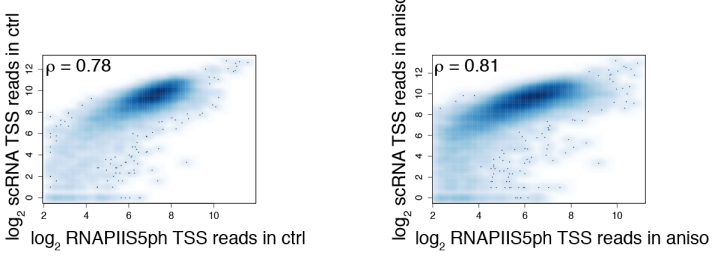

E

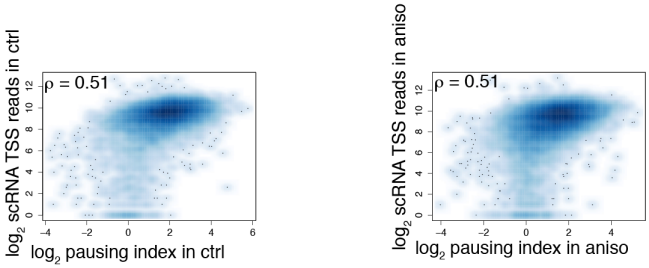

Sawicka_Suppl_Fig13

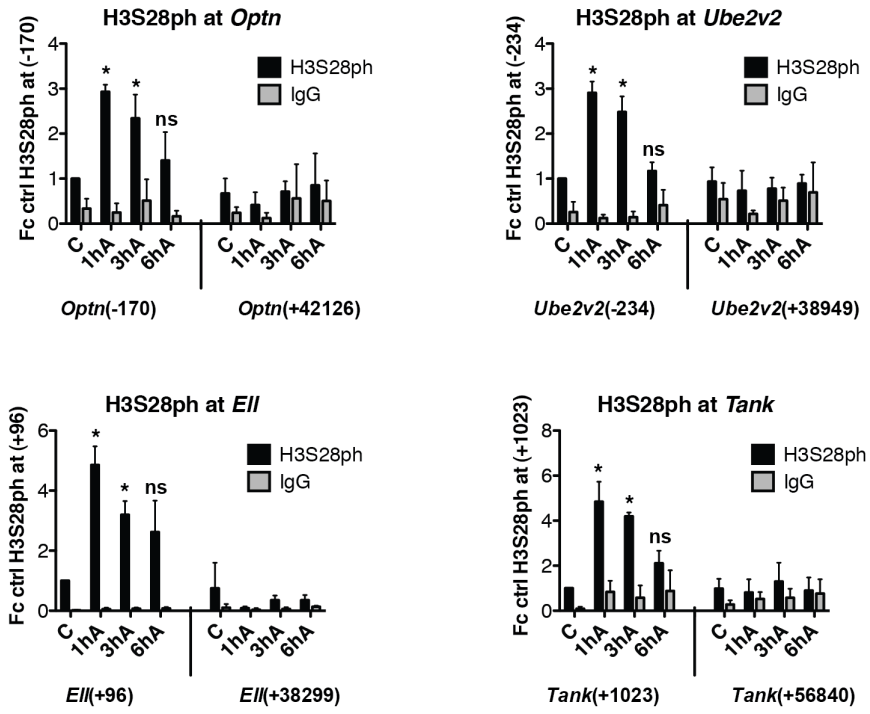

Sawicka_Suppl_Fig14

A

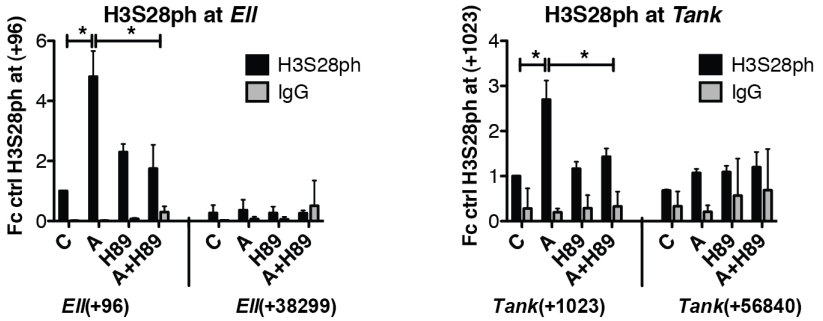

B

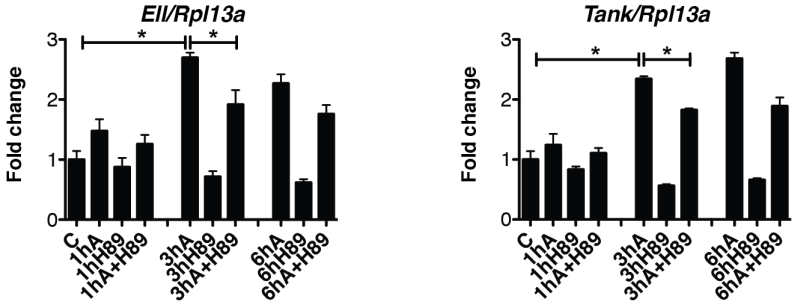

Sawicka_Suppl_Fig15

RPKM/transcript in ctrl mRNA-seq

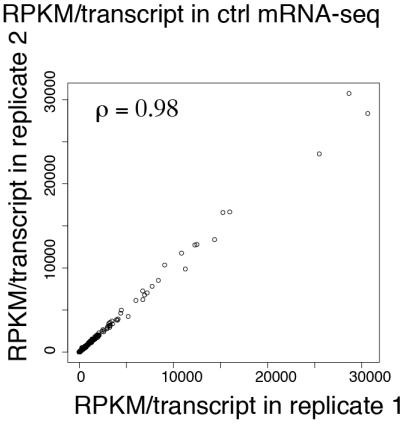

RPKM/transcript in 3hA mRNA-seq

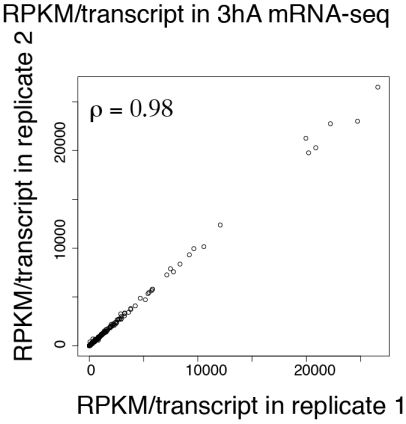

RPKM/transcript in 3hA+H89 mRNA-seq

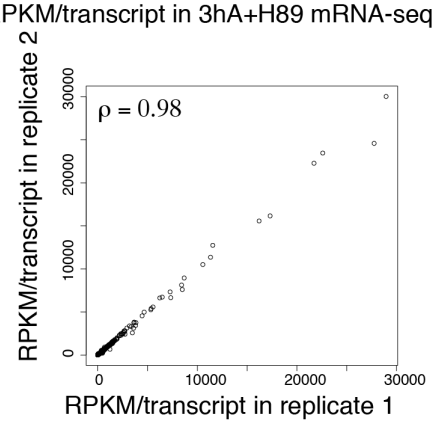

RPKM/transcript in 3hH89 mRNA-seq

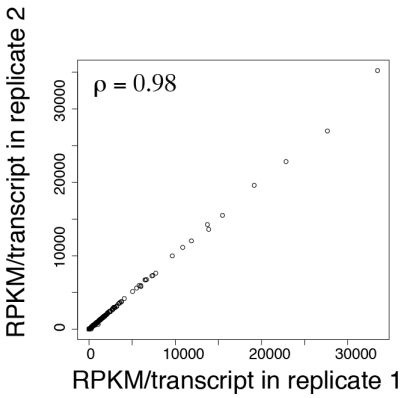

RPKM/transcript in 6hA mRNA-seq

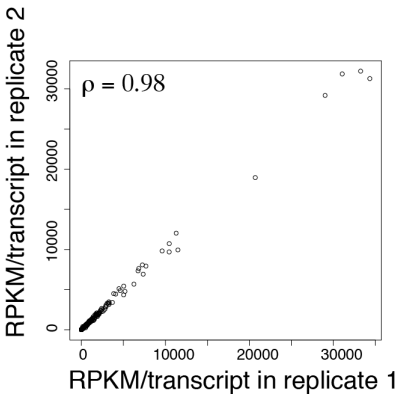

RPKM/transcript in 6hA+H89 mRNA-seq

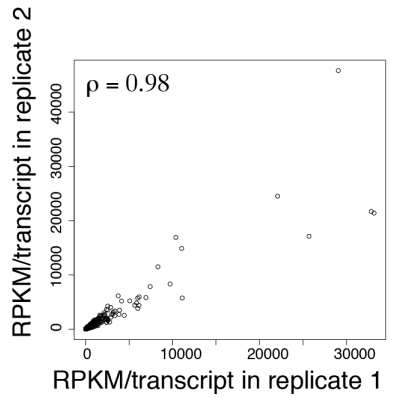

RPKM/transcript in 6hH89 mRNA-seq

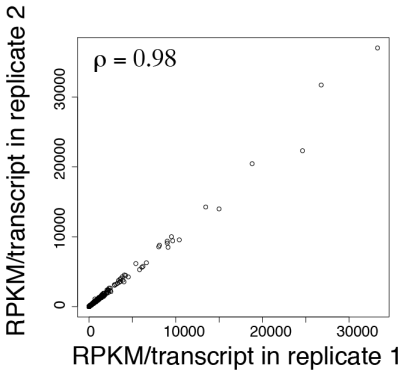

Sawicka_Suppl_Fig16

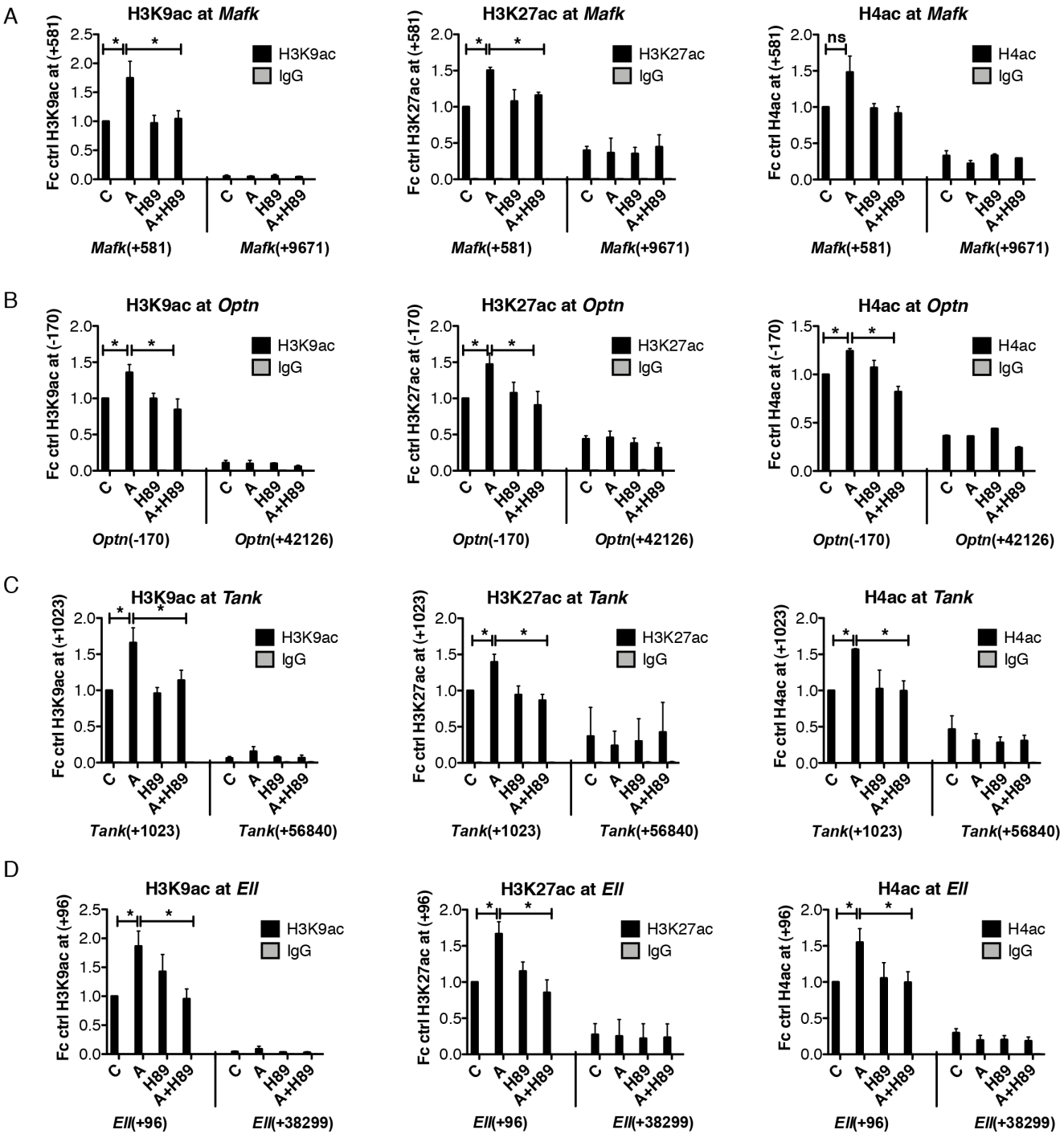

Sawicka_Suppl_Fig17

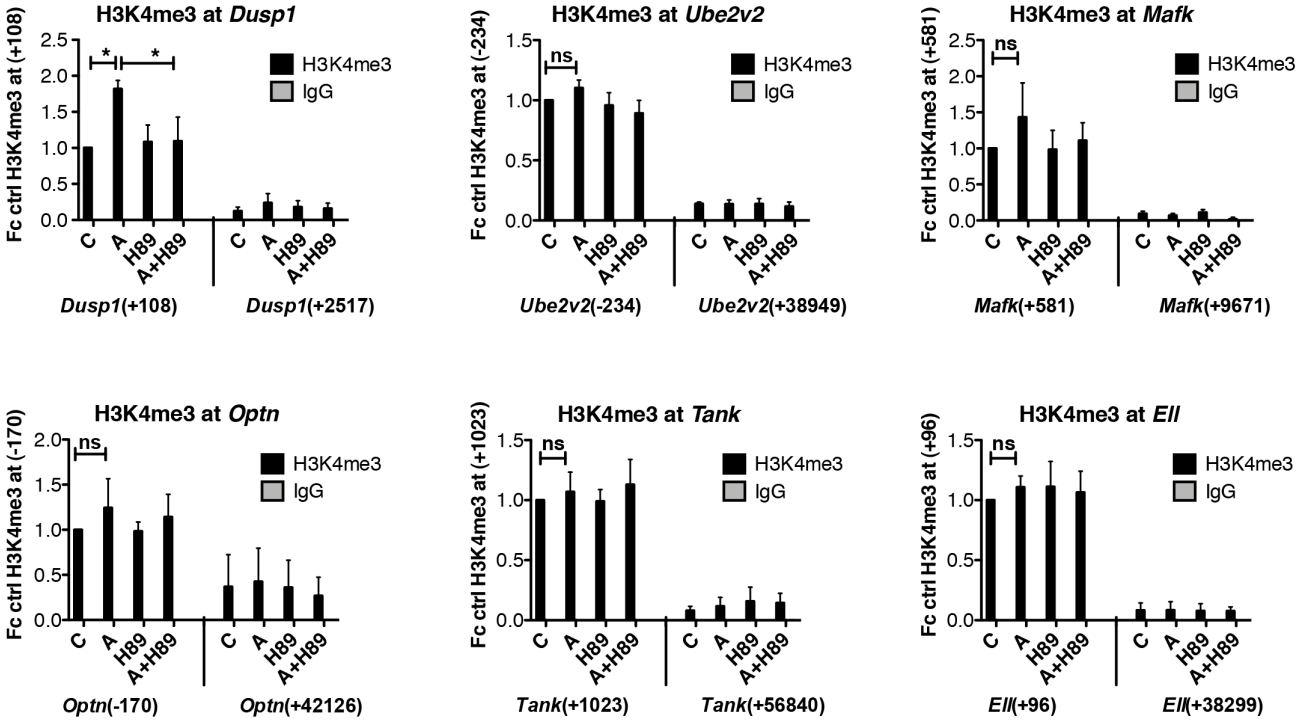

Sawicka_Suppl_Fig18

		number of identified peptides		
Protein	**Accession**	**H3(19-36)unmodified**	**H3(19-36)H3S28ph**	
14-3-3 zeta/delata	gil52000886	0	14	**14-3-3 proteins**
14-3-3 epsilon	gil51702210	0	12	
14-3-3 beta/alpha	gil1345590	0	10	
14-3-3 gamma	gil48428718	0	9	
14-3-3 eta	gil1345593	0	9	
14-3-3 theta	gil112690	2	9	
14-3-3 sigma	gil398953	0	5	
SIN3A	gil37999759	4	0	**Sin3A complex**
SUDS3	gil68053233	2	0	
SAP18	gil6831678	3	0	
ARID4B	gil143955276	2	0	
SAP30BP	gil74761958	3	2	
GATAD2A	gil50401012	2	0	
CHD4	gil311033360l	6	0	**NuRD complex**
MBD3	gil50400820	2	0	
MTA2	gil29840793	7	0	
RBBP7	gil2494891	6	2	**Sin3A/NuRD complex**

Sawicka_Suppl_Fig19

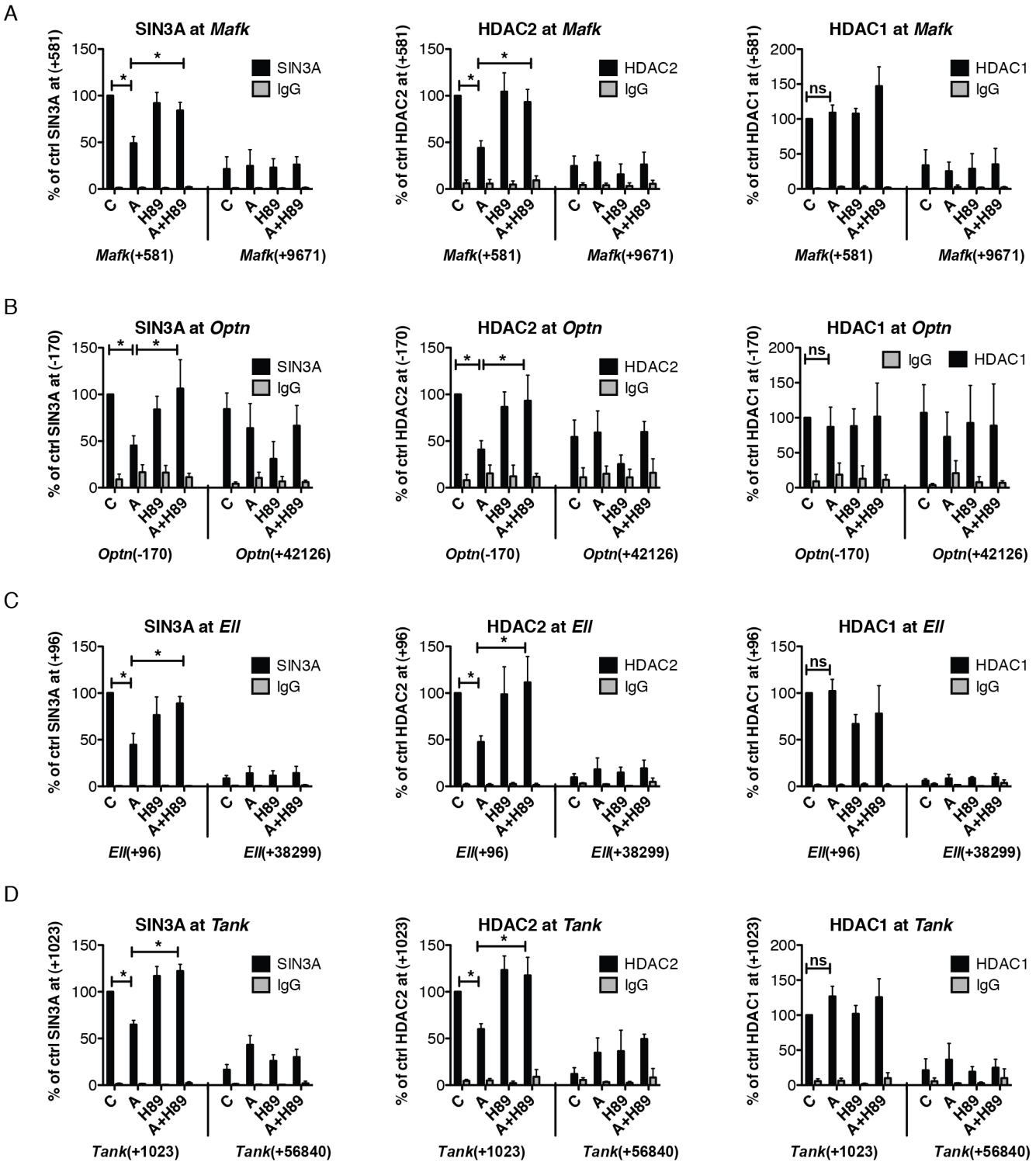

Sawicka_Suppl_Fig20

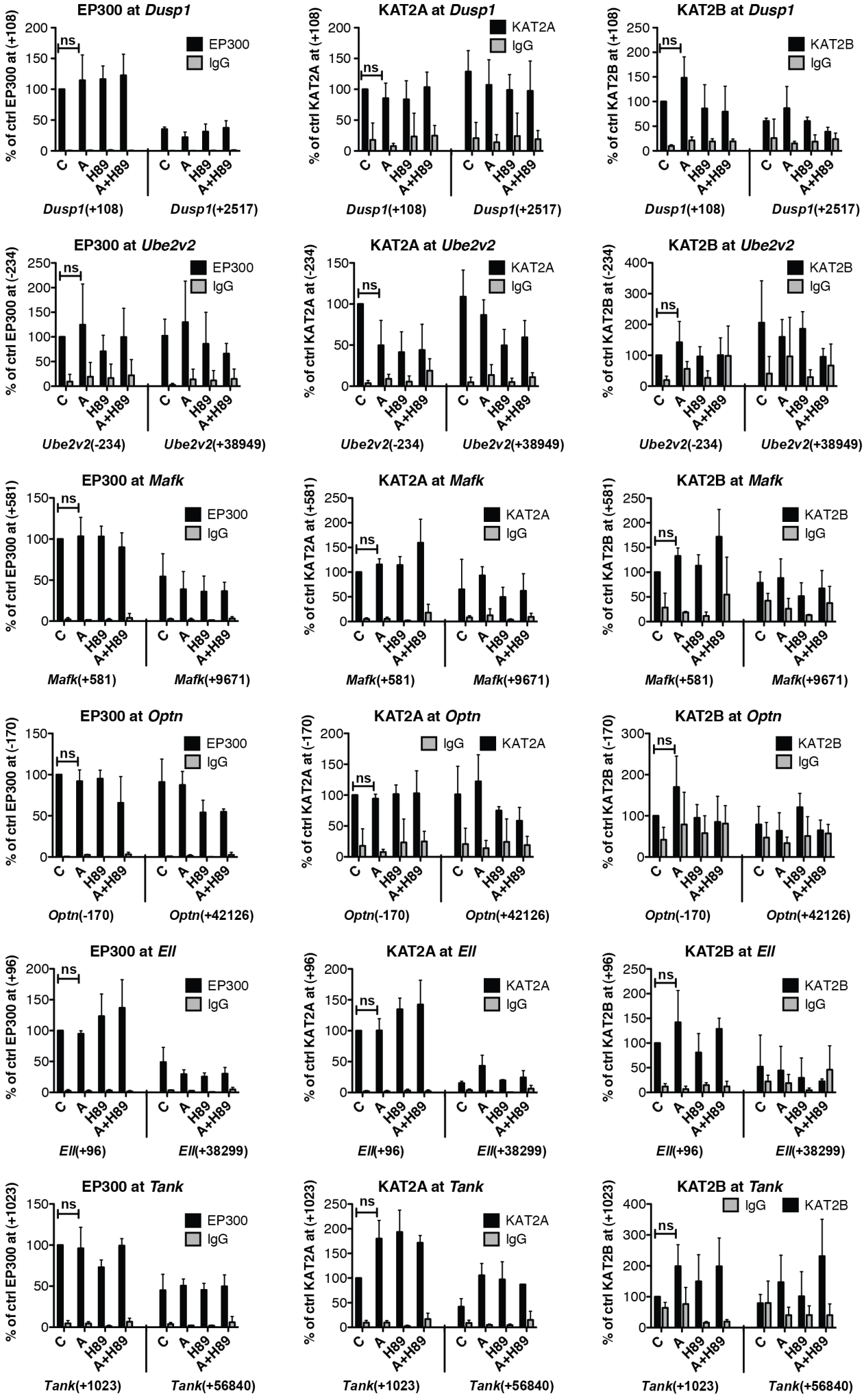

Sawicka_Suppl_Fig21

A

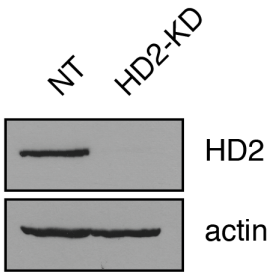

B

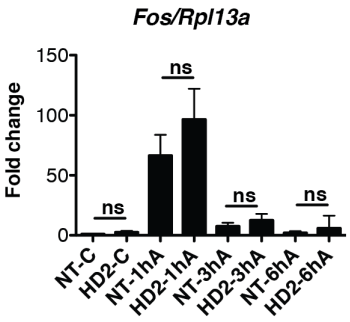

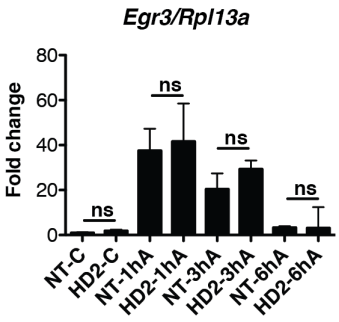

C